Containerless Rapid Solidification of Liquid Ti-Al-V Alloys Inside Drop Tube

Chapter · May 2016
DOI: 10.1002/9781119296126.ch62

6 authors, including:

Shaolou Wei
Massachusetts Institute of Technology
12 PUBLICATIONS **23** CITATIONS
SEE PROFILE

L.J. Huang
Harbin Institute of Technology
99 PUBLICATIONS **1,387** CITATIONS
SEE PROFILE

Y. H. Wu
Northwestern Polytechnical University
19 PUBLICATIONS **40** CITATIONS
SEE PROFILE

Shangjing Yang
Northwestern Polytechnical University
19 PUBLICATIONS **40** CITATIONS
SEE PROFILE

PROCEEDINGS OF THE 13TH
WORLD CONFERENCE ON TITANIUM

Melting and Casting II

Proceedings of the 13th World Conference on Titanium
Edited by: Vasisht Venkatesh, Adam L. Pilchak, John E. Allison, Sreeramamurthy Ankem, Rodney Boyer, Julie Christodoulou, Hamish L. Fraser, M. Ashraf Imam, Yoji Kosaka, Henry J. Rack, Amit Chatterjee, and Andy Woodfield
TMS (The Minerals, Metals & Materials Society), 2016

CONTAINERLESS RAPID SOLIDIFICATION OF LIQUID Ti-Al-V ALLOYS INSIDE DROP TUBE

S.L. Wei[1], L.J. Huang[1,*], J. Chang[2], S.J. Yang[2], Y.T. Ma[1], L. Geng[1]
[1]School of Materials Science and Engineering, Harbin Institute of Technology, Harbin , 150001, China
[2]School of Natural and Applied Sciences, Northwestern Polytechnical University, Xian 710072, China
[*]Corresponding author: huanglujun@hit.edu.cn

A short drop tube with 3m length and 10^{-3}g gravity was applied to realize the containerless rapid solidification of liquid Ti-6Al-4V, Ti-18Al-12V and Ti-30Al-20V alloys. The diameters of alloy droplets ranged from 65 to 1510μm, which corresponded to the cooling rates of 10^3 ~10^5 K/s and the undercooling levels of 200~700K. Bulk TC4 alloy melt was also undercooled by electromagnetic levitation technique and achieved a maximum undercooling of 208K ($0.11T_L$). The primary β phase usually grew in dendritic mode and then decomposed into basket weave microstructures, but sometimes was retained to ambient temperature at sufficiently high cooling rate. The microstructural evolution mechanisms were explored theoretically with the aids of SEM analyses.

Keywords: rapid solidification, Ti-Al-V alloy, high undercooling, drop tube, microgravity, dendritic growth

1. Introduction

Titanium based alloys have become the important structural materials in aerospace industry and related engineering fields for over half century. Owing to the wide applications of TC4 alloy, ternary Ti-Al-V alloy system attracts great research interest for both fundamental and applied research [1-3]. Directional solidification technique is frequently applied to grow single crystal alloys and explore solidification mechanisms[4-6]. Whereas the rapid solidification of Ti-based alloys are usually realized by rapid quenching techniques. Because of their high chemical reactivity at elevated temperatures, it is very difficult to undercool bulk liquid titanium and its alloys under conventional melting and casting conditions. Fortunately, it is found that electromagnetic levitation technique offers an effective approach to avoid heterogeneous nucleation and hence undercool Ti alloy melts to a large extent[7-10].

The containerless solidification processing of liquid alloys inside drop tube provides the combined advantages of high undercooling, rapid quenching and microgravity state. This opens a new approach to experimentally investigate the nonequilibrium solidification mechanisms of Ti-based alloys. Although there have been numerous investigations on the rapid solidification of titanium alloys, much work remains to be done concerning the crystallization kinetics of substantially undercooled alloy melts. In particular, a quantitative attempt to describe the nucleation process at containerless state is highly desirable. The objective of the present research is to investigate the undercoolablity, nucleation characteristics and microstructural evolution of three Ti-Al-V alloys with the same Al/V ratio of 3/2. A comparison is also made between drop tube processing and electromagnetic levitation technique in order to reveal their possible differences in rapid solidification kinetics.

2. Experimental Procedure

As illustrated in Fig.1 where the phase diagram was cited from reference [1], three alloys with the same Al/V ratio of 3/2, that is Ti-6wt%Al-4wt%V, Ti-18wt%Al-12wt%V and Ti-30wt%Al-20wt%V, were selected for experimental study. The master alloys were all prepared from 99.99% pure Ti, 99.999% pure Al and 99.8% pure V with a high vacuum arc melting furnace. Each prealloy sample for drop tube experiment weighed 1g, while that for electromagnetic levitation experiment had a weight of 0.5g.

A drop tube with a height of 3m and an inner diameter of 150mm was applied to realize the containerless rapid solidification of these Ti-Al-V alloys through the free falling of their droplets. It firstly achieved a vacuum of 5×10^{-5} Pa and was then refilled with 1atm argon gas, which provided a reduced gravity level of about 10^{-3} g_o for the falling alloy droplets. A quartz tube with the size of 13mm ID × 15mm OD × 160mm contained the master alloy sample and was installed on the top of drop tube. It had a 0.2mm diameter orifice at its bottom for the purpose of spraying and atomizing the molten bulk alloy. The prealloy sample was melted by radio frequency induction heating, superheated to 100K above its liquidus temperature and finally ejected through the orifice into a great number of freely falling droplets.

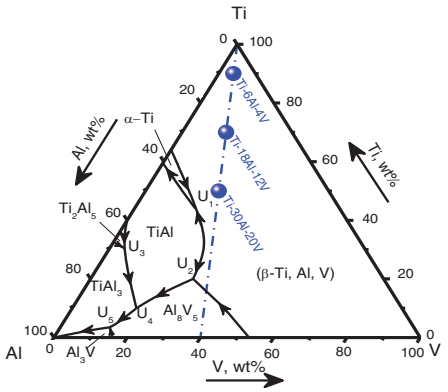

Fig. 1 Selection of three alloy compositions in phase diagram.

As a comparative approach to accomplish containerless processing, liquid Ti-6Al-4V alloy was also undercooled and subsequently solidified by electromagnetic levitation technique. In this latter case, the vacuum level was 10^{-5} Pa and the superheating of liquid alloy attained 200-350K. The levitated liquid alloy was cooled down by a flow of refrigerated helium gas and its temperature was monitored by an infrared pyrometer with 0.2% accuracy. After experiments, all the samples were sectioned, polished and etched with an aqueous solution of HF + HNO_3. An FEI Sirion electron microscope together with INCA Energy 300 energy dispersive spectrometer was utilized to explore the phase constitution and microstructural morphologies of the containerlessly solidified Ti-Al-V alloys.

3. Results and Discussion

3.1 Rapid cooling of alloy droplets

The atomization of bulk liquid Ti-Al-V alloys was accomplished by the Rayleigh instability of freely falling melt column after the ejecting from the small orifice at quartz tube bottom. Therefore, the size of alloy droplets depends mainly upon the melt surface tension and viscosity as well as the orifice diameter and the ejecting Ar gas pressure. Alloy droplets become spherical shape as soon as isolated from the sprayed melt flow. For Ti-6Al-4V alloy, SEM observations indicate that droplet diameters range from 327 to 1130μm.

An alloy droplet falling freely within the Ar atmosphere inside drop tube is cooled down by both thermal radiation and thermal convection. Its cooling rate R_c is determined by the following heat balance equation:

$$R_c = \frac{6[\varepsilon_L \sigma_{SB}(T^4 - T_0^4) + h(T - T_0)]}{\rho_L C_{PL} D} \quad (1)$$

where ε_L is the radiation emissivity of liquid alloy, σ_{SB} the Stefan-Boltzman constant $5.67\times10^{-8}W/m^2K^4$, T the temperature of alloy droplet, T_o the temperature of surroundings 298K, h the heat transfer coefficient between alloy droplet and argon, ρ_L the density of liquid alloy, C_{PL} the specific heat of liquid alloy, and D the diameter of alloy droplet. When a spherical droplet is moving inside a gas atmosphere, their heat transfer coefficient h of thermal convection can be derived by the following characteristic equation[11]:

$$N_u = 2 + 0.6\, R_e^{1/2} P_r^{1/3} \quad (2)$$

in which N_u is the Nusselt number hD/λ_o , R_e the Reynold number $\upsilon_r\rho_o D/\eta_o$, and P_r the Prandtl number $\eta_o C_{Po}/\lambda_o$. Here ρ_o, η_o, λ_o and υ_r represent the gas density, viscosity, thermal conductivity and the moving velocity of alloy droplet relative to surrounding gas.

According to Equ.s (1) and (2), the cooling rate of an alloy droplet varies mainly with its diameter, temperature and velocity. Fig.2 presents the calculated cooling rates for Ti-6Al-4V alloy droplets, where their initial falling velocity is presumed as 1m/s. As seen in

Fig.2(a), at the superheating of 100K, the smallest alloy droplet with 327μm diameter achieves a cooling rate of 7.64×10^3K/s, whereas the largest alloy droplet with 1130μm diameter cools down at a rate of 1.21×10^3K/s. On the other hand, their cooling rates slow down as the temperatures of alloy droplets decrease gradually. Fig.2(b) demonstrates that the cooling rate of the smallest alloy droplet reduces from 6.64×10^3 to 4.03×10^3K/s when its temperature falls from the liquidus 1933 to 1500K. Since there are only limited differences for the relevant physical parameters of Ti-18Al-12V and Ti-30Al-20V alloys, they display similar cooling rates with the same order of magnitude as compared with Ti-6Al-4V alloy.

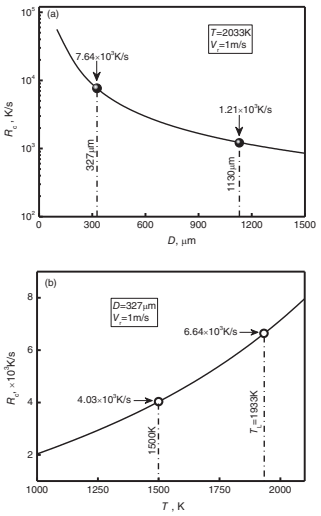

Fig. 2 Calculated cooling rate for Ti-6Al-4V alloy droplet: (a) versus diameter, and (b) versus temperature.

3.2 Nucleation of primary β phase

The solidification process of Ti-Al-V alloy droplets inside drop tube is characterized by containerless state, rapid cooling and microgravity environment. As can be judged from Fig.1, the keynote of the solidification process for the selected three alloys is the formation of primary β-(Ti, Al, V) phase, which is a bcc structured Ti solid solution phase dissolving Al and V solutes. It is apparent that the containerless processing by drop tube may prevent the heterogeneous nucleation of primary β phase to a great extent and lead to a large degree of undercooling. Nevertheless, its homogeneous nucleation is still not guaranteed because the inherent impurities within liquid alloys cannot be eliminated completely.

In the light of classic nucleation theory [12], the nucleation rate I of β phase in liquid Ti-Al-V alloys is determined by the following relation:

$$I = I_0 \exp\left(-\frac{\Delta G^* f(\theta)}{k_B T}\right)\exp\left(-\frac{Q}{k_B T}\right) \tag{3}$$

Here $f(\theta)=(2+\cos\theta)(1-\cos\theta)^2/4$ is the catalytic potency factor of heterogeneous nucleus with wetting angle θ. ΔG* stands for the thermodynamic activation energy of nucleation, Q the activation energy of atomic diffusion in liquid alloy, T the temperature of liquid alloy, I_o the nucleation prefactor 10^{41}m^{-3}s^{-1}, k_B the Boltzmann constant 1.38×10^{-23}J/K.

The critical condition to initiate the solidification of a Ti-Al-V alloy droplet with volume V is that at least one nucleus is formed in the allowable period of cooling time t, which is IVt≥1. If coupled with Equ (3), this marginal situation can be further described as below:

$$f(\theta) \le \frac{k_B T \ln(I_0 V t) - Q}{\Delta G^*} \tag{4}$$

The above two equations establish the interrelation between the nucleation rate of primary β phase and the undercooling of alloy melt together with the wetting angle of emerging nucleus on heterogeneous substrate.

Due to their small size and fast moving velocity, the actual undercooling of Ti-Al-V alloy droplets is difficult to measure directly during their free fall inside drop tube. Meanwhile, it is even more impossible to detect the wetting angle θ of primary β phase upon heterogeneous nucleus. In contrast, electromagnetic levitation processing has the advantage that the undercooling of levitated alloy drop can be accurately measured by infrared pyrometry. Thus the wetting angle is predicted by Equ (5) if this kind of levitation experiments is performed. Fig.3 gives the rapid solidification microstructures of electromagnetically levitated Ti-6Al-4V alloy, where the sample is almost spherical and has a diameter of 6mm. Obviously, the formation of primary β phase dominates the solidification process in such a way that there are no traces of those subsequent monavariant reactions designated in Fig.1. But it has completely transformed

into very fine and uniform lamellar α phase structures after solidification. The maximum undercooling of levitated bulk alloy melt attains 208K($0.11T_L$), while its cooling curve indicates that containerless solidification process lasts for only 1s. Combining these experimental results with Equ.(5), it is inferred that the wetting angle of primary β phase is $\theta \geq 56^o$. Because the master alloys are prepared from the identically high purity elements and through the exactly same melting procedure, it is reasonable to assume that the Ti-6Al-4V alloy droplets hold the similar wetting angle for primary β phase during the containerless solidification inside drop tube.

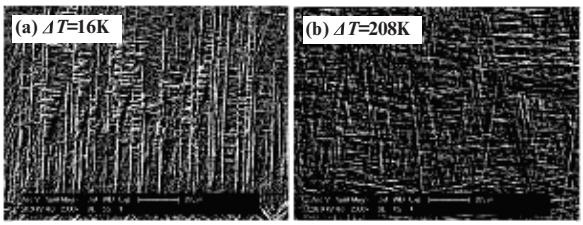

Fig. 3 Microstructures of EML levitated Ti-6Al-4V alloy versus undercooling: (a) 16 K, (b) 208K.

The calculated results of nucleation process for primary β phase in Ti-6Al-4V alloy droplets within drop tube are illustrated in Fig.4. Evidently, the thermodynamic driving force for crystallization ΔG_{LS}, which is the Gibbs free energy difference between liquid and solid phase, increases linearly with the undercooling of alloy melt. In the meanwhile, the activation energy of nucleation ΔG*, which is the thermodynamic barrier against nucleation resulting from solid-liquid interfacial energy, decreases with the rise of alloy droplet undercooling. Fig.4(b) provides the calculated heterogeneous and homogeneous nucleation rates versus undercooling. As the most conservative assumption, the total free falling time of 0.78s inside the 3m high drop tube is taken as the solidification time of alloy droplets. Thus, the largest alloy droplet with 1130μmdiameter needs an undercooling of 217K to ensure that at least one nucleus is formed through heterogeneous nucleation. As a contrast, a much larger undercooling of 750K is necessary for the homogeneous nucleation of primary β phase. In the case of the smallest alloy droplet with 327μm diameter, the critical undercoolings for heterogeneous and homogeneous nucleation are 223 and 784K respectively. Its actual nucleation rates lie in the shadowed regime of Fig.4(b).

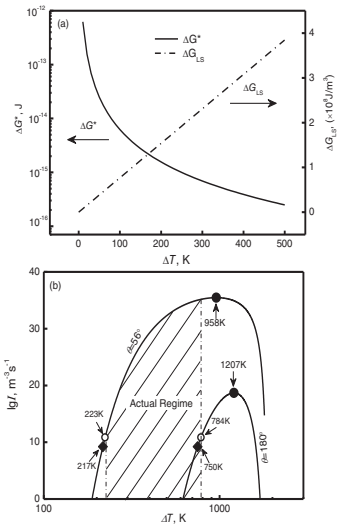

Fig. 4 Nucleation kinetics of undercooled liquid Ti-6Al-4V alloy: (a) thermodynamic barrier and driving force for crystallization, (b) heterogeneous and homogeneous nucleation rates.

3.3 Structures of rapidly solidified Ti-Al-V alloys

According to the ternary phase diagram shown in Fig.1, the solidification process of the three selected Ti-Al-V alloys begins with the nucleation and growth of primary β phase. At the later stage of solidification, there are two probable monavariant reactions and one invariant reaction for the residue alloy melt: L→α+β, L→β+γ, and L+β→α+γ.

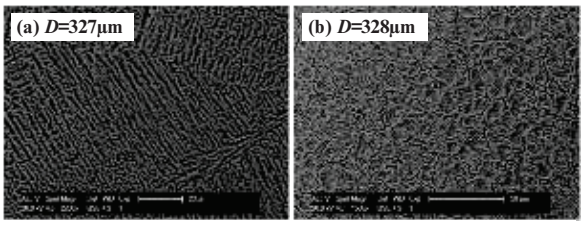

Fig. 5 Microstructures of small Ti-6Al-4V alloy droplets: (a) fine dendrites of 327μm droplet, (b) equiaxed grains of 328μm droplet.

SEM analyses have revealed that there are three types of microstructures for containerlessly solidified Ti-6Al-4V alloy. As seen in Fig.5, for those small alloy droplets with diameters below 400μm, the metastable β phase dendrites or equiaxed grains are characteristic of the rapid solidification microstructures. It is notable

that the high cooling rate suppresses the decomposition of β phase and retains it until ambient temperature. In the intermediate diameter range of 674-855μm, the basket weave microstructures illustrated in Fig.6(a) are formed through the decomposition of β phase after solidification. This is similar to the microstructures yielded by containerlees solidification with electromagnetic levitation technique demonstrated in Fig.3. As for the large alloy droplets with 944-1130μm diameter, the relatively complete decomposition of β phase results in the lamellar microstructures presented in Fig.6(b). It deserves to mention that no hints are found for the possible monavariant and invariant reactions in this alloy.

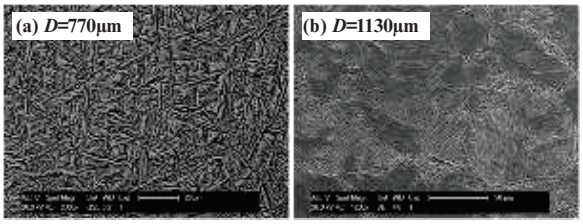

Fig. 6 Morphologies of large Ti-6Al-4V alloy droplets : (a) basket weave structures of 770μm droplet, and (b) lamellar structures of 1130μm droplet.

The diameters of Ti-18Al-12V alloy droplets vary from 65 to 1510μm. Fig.7 provides the containerless solidification microstructures of this alloy versus droplet diameter. Since the increase of V content effectively stabilizes the primary β phase, it is easily retained to ambient temperature without decomposition in the broad diameter range below 469μm. As shown in Fig.7(a), the metastable β phase appears as very fine equiaxed dendrites in the small alloy droplet with 89μm diameter. Fig.7(b) displays that well branched dendrites are the typical morphology of metastable β phase in the medium sized alloy droplet with 469μm diameter. Concerning the large alloy droplets with 883-1510μm diameters, basket weave structures are the main feature of their metallographic morphology, which is clearly illustrated in Fig.7(c). If compared with the microstructures of Ti-6Al-4V alloy given in Fig.6, it is apparent that only partial decomposition occurs to the primary β phase owing to the stabilization effect of increased V content. Similarly, the probable monavariant and invariant reactions do not take place in this alloy.

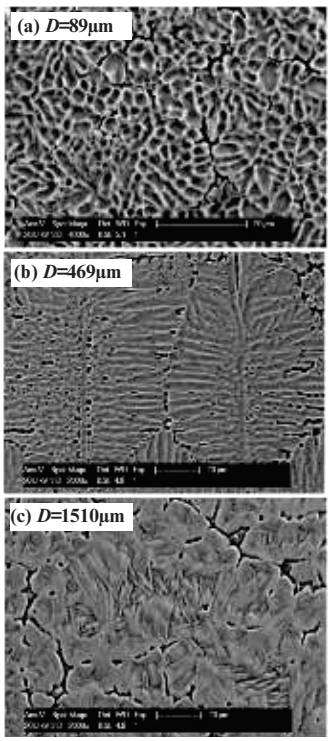

Fig. 7 Microstructures of Ti-18Al-12V alloy droplets: (a) equiaxed dendrites of 89μm droplet, (b) columnar dendrites of 469μm droplet, (c) basket weave structures of 1510μm droplet.

The highly concentrated Ti-30Al-20V alloy exhibits a droplet diameter range of 155--1210μm during containerless processing inside drop tube. The enhanced V content tends to stabilize the primary β phase, whereas the high Al content increases the stability of α phase. In fact, some peculiarities do appear in this alloy. Firstly, the solidification pathway shows a certain kind of new feature. Secondly, its corrosion resistance is greatly raised as compared with the other two Ti-Al-V alloys, which is revealed by the etching procedure of metallographic analyses. As demonstrated by Fig.8(a), in the small alloy droplets with 155-554μm diameters, their microstructures consist of γ-TiAl compound plus matrix β phase. This indicates that the monavariant reaction L→β+γ may have happened after the formation of primary β phase during the containerless solidification of these small droplets. For the large alloy droplets with 924-1210μm diameters, the refined basket weave structures shown in Fig.8(b) have evolved from the partial

decomposition of primary β phase.

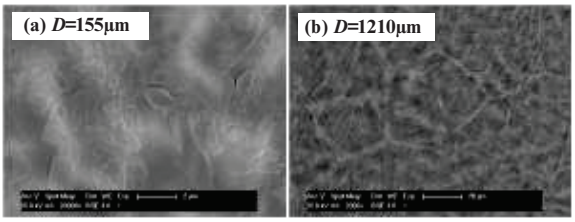

Fig. 8 Structures of Ti-30Al-20V alloy droplets: (a) γ phase distributed in β matrix of 155μm droplet, and (b) basket weave structures of 1210μm droplet.

4. Conclusions

In summary, three liquid Ti-Al-V alloys with the same Al/V ratio of 3/2 have been highly undercooled and rapidly solidified inside drop tube. As a comparison, the Ti-6Al-4V alloy was also containerlessly solidified by electromagnetic levitation technique. The main findings are as follows:

(1) A maximum undercooling of 208K($0.11T_L$) was obtained for liquid Ti-6Al-4V alloy at electromagnetic levitation state. This indicates that most of the inherent heterogeneous nuclei within alloy melt have wetting angles above 56°.

(2) The alloy droplets display a diameter range of 65-1510μm, corresponding to the cooling rates of 10^5-10^3K/s. Meanwhile, they can achieve high undercoolings of 200—700K during free falling.

(3) Both Ti-6Al-4V and Ti-18Al-12V alloys hold metastable β phase dendrites and equiaxed grains at ambient temperature, if alloy droplets are sufficiently small. Whereas basket weave or lamellar structures are formed through the decomposition of primary phase for large alloy droplets. No monavariant and invariant reactions take place in these two alloys.

(4) Ti-30Al-20V alloy shows refined basket weave microstructures when its droplet diameters are large enough. The enhancement of alloy undercooling and cooling rate results in the occurrence of a subsequent monavariant reaction after the formation of primary β phase.

Acknowledgements

The authors are grateful to Assoc. Prof. W. Zhai and Mr. Y. H. Wu for their help with the experiments and analyses. This work was financially supported by National Natural Science Foundation of China under grant No.s 51471063, 51271064 and 51401167 as well as the Scientific Innovation Program for Students of Harbin Institute of Technology under grant No. F19002.

REFERENCES

[1] H.Wang, N.Warnken and R.C.Reed, Mat.Sci.Eng.A, 2010, 528: 622-630.

[2] R.Srinivasan and S.Tamirisakandala, Scr. Mater., 2010, 63: 1244-1247.

[3] L.J.Xu et al, Trans. Nonferrous Met. Soc. China, 2012, 22: 768-772.

[4] X.F.Ding et al, Acta Mater., 2012, 60: 498-506.

[5] H.N.Lee et al, Acta Mater., 2000, 48: 3221-3233.

[6] J.L.Fan et al, J. Alloys Compd, 2010, 504: 60-64.

[7] C.D.Anderson, W.H.Hofmeister and R.J.Bayuzick, Metall. Trans A., 1992, 23A: 2699-2714.

[8] K.Zhou, H.P.Wang and B.Wei, Chem. Phys. Lett., 2012, 521: 52-54.

[9] O.Shuleshova et al, Acta Mater., 2007, 55: 681-689.

[10] Y.C.Liu et al, Mat. Lett., 2004, 58: 428-431.

[11] K.Wu, Transport *Principles of Metallurgical Processes* (Beijing, Metallurgical Industry Press, 2011), 169-178.

[12] W.Kurz and D.J.Fisher, *Fundamentals of Solidification* (Switzerland, Trans Tech Publications Ltd, 1998), 22-33.